SANTA CRUZ BIOTECHNOLOGY, INC.

ALDH1/2 (H-8): sc-166362

SANTA CRUZ BIOTECHNOLOGY

The Power to Question

BACKGROUND

Aldehyde dehydrogenases (ALDHs) mediate $NADP^+$-dependent oxidation of aldehydes into acids during the detoxification of alcohol-derived acetaldehyde; metabolism of corticosteroids, biogenic amines and neurotransmitters; and lipid peroxidation. ALDH1A1, also designated retinal dehydrogenase 1 (RalDH1 or RALDH1), aldehyde dehydrogenase family 1 member A1, aldehyde dehydrogenase cytosolic, ALDHII, ALDH-E1 or ALDH E1, is a retinal dehydrogenase that participates in the biosynthesis of retinoic acid (RA). The major liver isoform ALDH1 localizes to cytosolic space, while ALDH2 localizes to the mitochondria. The ALDH1A2 (RALDH2, RALDH2-T) gene produces three different transcripts and also catalyzes the synthesis of RA from retinaldehyde. ALDH2 is present in most Caucasians, yet is absent in 50% of Asians. The absence of this enzyme has been linked to alcohol intolerance and, thusly, a reduced risk for alcoholism-related liver disease.

SOURCE

ALDH1/2 (H-8) is a mouse monoclonal antibody raised against amino acids 186-270 mapping within an internal region of ALDH1A1 of human origin.

PRODUCT

Each vial contains 200 µg IgG_{2b} kappa light chain in 1.0 ml of PBS with < 0.1% sodium azide and 0.1% gelatin.

ALDH1/2 (H-8) is available conjugated to agarose (sc-166362 AC), 500 µg/ 0.25 ml agarose in 1 ml, for IP; to HRP (sc-166362 HRP), 200 µg/ml, for WB, IHC(P) and ELISA; to either phycoerythrin (sc-166362 PE), fluorescein (sc-166362 FITC), Alexa Fluor® 488 (sc-166362 AF488), Alexa Fluor® 546 (sc-166362 AF546), Alexa Fluor® 594 (sc-166362 AF594) or Alexa Fluor® 647 (sc-166362 AF647), 200 µg/ml, for WB (RGB), IF, IHC(P) and FCM; and to either Alexa Fluor® 680 (sc-166362 AF680) or Alexa Fluor® 790 (sc-166362 AF790), 200 µg/ml, for Near-Infrared (NIR) WB, IF and FCM.

Alexa Fluor® is a trademark of Molecular Probes, Inc., Oregon, USA

APPLICATIONS

ALDH1/2 (H-8) is recommended for detection of ALDH1A1, ALDH1A2, ALDH1A3 and ALDH2 of mouse, rat and human origin by Western Blotting (starting dilution 1:100, dilution range 1:100-1:1000), immunoprecipitation [1-2 µg per 100-500 µg of total protein (1 ml of cell lysate)], immunofluorescence (starting dilution 1:50, dilution range 1:50-1:500), immunohistochemistry (including paraffin-embedded sections) (starting dilution 1:50, dilution range 1:50-1:500) and solid phase ELISA (starting dilution 1:30, dilution range 1:30-1:3000).

Molecular Weight of ALDH1/2: 53 kDa.

Positive Controls: mouse liver extract: sc-2256, Hep G2 cell lysate: sc-2227 or A549 cell lysate: sc-2413.

STORAGE

Store at 4° C, **DO NOT FREEZE**. Stable for one year from the date of shipment. Non-hazardous. No MSDS required.

RESEARCH USE

For research use only, not for use in diagnostic procedures.

DATA

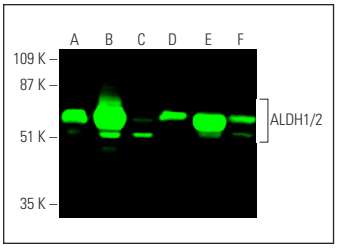

ALDH1/2 (H-8): sc-166362. Near-infrared western blot analysis of ALDH1/2 expression in Hep G2 (**A**), A549 (**B**) and Caki-1 (**C**) whole cell lysates and human skeletal muscle (**D**), mouse liver (**E**) and human brain (**F**) tissue extracts. Blocked with UltraCruz® Blocking Reagent: sc-516214. Detection reagent used: m-IgGκ BP-CFL 680: sc-516180.

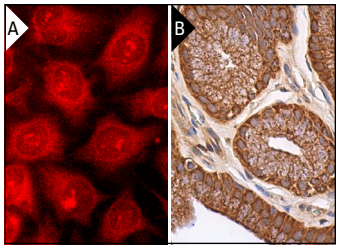

ALDH1/2 (H-8): sc-166362. Immunofluorescence staining of methanol-fixed HeLa cells showing cytoplasmic localization (**A**). Immunoperoxidase staining of formalin fixed, paraffin-embedded human gall bladder tissue showing cytoplasmic staining of glandular cells (**B**).

SELECT PRODUCT CITATIONS

1. Pizzi, S. 1989. Presentation of the graduate course in odontology and dental prosthetics. Acta Biomed. Ateneo Parmense 60: 37-41.
2. Xie, M.Q., et al. 2011. Modulation of immune tolerance with a Chinese traditional prescription inhibits allergic rhinitis in mice. N. Am. J. Med. Sci. 3: 503-507.
3. Chandrasekaran, S., et al. 2014. TRAIL-mediated apoptosis in breast cancer cells cultured as 3D spheroids. PLoS ONE 9: e111487.
4. Demirayak, B., et al. 2016. Effect of bone marrow and adipose tissue-derived mesenchymal stem cells on the natural course of corneal scarring after penetrating injury. Exp. Eye Res. 151: 227-235.
5. Kumar, V., et al. 2017. Design, synthesis and biological evaluation of novel hedgehog inhibitors for treating pancreatic cancer. Sci. Rep. 7: 1665.
6. Laranjo, M., et al. 2018. Mammospheres of hormonal receptor positive breast cancer diverge to triple-negative phenotype. Breast 38: 22-29.
7. Shishido, A., et al. 2018. Mesothelial cells facilitate cancer stem-like properties in spheroids of ovarian cancer cells. Oncol. Rep. 40: 2105-2114.
8. Parte, S.C., et al. 2018. Characterization of stem cell and cancer stem cell populations in ovary and ovarian tumors. J. Ovarian Res. 11: 69.
9. Xiong, Q., et al. 2018. BMP-2 inhibits lung metastasis of osteosarcoma: an early investigation using an orthotopic model. Onco Targets Ther. 11: 7543-7553.
10. Carvalho, M.J., et al. 2019. Endometrial cancer spheres show cancer stem cells phenotype and preference for oxidative metabolism. Pathol. Oncol. Res. 25: 1163-1174.

PROTOCOLS

See our web site at www.scbt.com for detailed protocols and support products.